NJC

Accepted Manuscript

This is an *Accepted Manuscript*, which has been through the Royal Society of Chemistry peer review process and has been accepted for publication.

Accepted Manuscripts are published online shortly after acceptance, before technical editing, formatting and proof reading. Using this free service, authors can make their results available to the community, in citable form, before we publish the edited article. We will replace this *Accepted Manuscript* with the edited and formatted *Advance Article* as soon as it is available.

You can find more information about *Accepted Manuscripts* in the Information for Authors.

Please note that technical editing may introduce minor changes to the text and/or graphics, which may alter content. The journal's standard Terms & Conditions and the Ethical guidelines still apply. In no event shall the Royal Society of Chemistry be held responsible for any errors or omissions in this *Accepted Manuscript* or any consequences arising from the use of any information it contains.

ROYAL SOCIETY OF CHEMISTRY

www.rsc.org/njc

Cite this: DOI: 10.1039/c0xx00000x

www.rsc.org/xxxxxx

Paper

Engineering lanthanide-optical centres in IRMOF-3 by post-synthetic modification

Reda M. Abdelhameed,[a,b] Luis D. Carlos,[c] Artur M. S. Silva,*[b] and João Rocha*[a]

Received (in XXX, XXX) XthXXXXXXXXX 20XX, Accepted Xth XXXXXXXXX 20XX

DOI: 10.1039/b000000x

The use of the post-synthetic modification of metal-organic frameworks is a recent strategy for engineering the coordination sphere of lanthanide cations and optimizing the light-emission properties of organic-inorganic hybrid materials. Here, IRMOF-3 was modified with 2-chloroacetic acid, glyoxylic acid, diethyl (ethoxymethylene)malonate and methyl vinyl ketone (vapour) and characterized by elemental analysis, solution and solid-state NMR, Fourier Transform Infrared spectroscopies, powder X-ray diffraction and scanning electron microscopy. The yields of the amino group's conversion were, respectively, 100% (IRMOF-3-CA), 75% (IRMOF-3-Gl), 80% (IRMOF-3-EM), and 76% (IRMOF-3-MVK). The reductive amination of IRMOF-3-Gl was carried out using sodium triacetoxyborohydride. The modified IRMOF-3 pendant groups were used to coordinate Eu^{3+} and Nd^{3+} and generating infrared (and visible) light emission.

Introduction

Metal Organic Frameworks (MOFs)[1-9] are very popular because, among other reasons, they are amenable to post-synthetic modification, that is, the organic linkers protruding into the nanochannels may undergo chemical reactions after the MOF's synthesis. For this to be possible, MOFs must be nanoporous, allowing the diffusion of reagents to the linker sites, chemically stable to the reaction media and incoming molecules.[9] The post-synthetic modification of MOFs has a number of advantages relatively to direct synthesis, such as the possibilities of controlling the type and number of functional groups that may be incorporated into the framework without affecting its stability, and of preparing topologically identical but functionally diverse frameworks. MOFs properties (*e.g.*, porosity, hydrophobicity, chemical stability, etc.) may be modulated and improved by post-synthetic modification[10] aiming at applications in gas sorption,[11] catalysis,[12] manipulating and monitoring reactions,[13] biomedicine,[14] and luminescence.[15]

Trivalent lanthanide (Ln^{3+}) ions are important light emitters employed in many applications ranging from laser lighting displays to optical telecommunication amplifiers.[16] The shielding of the 4f electrons by occupied $5s^2$ and $5p^6$ orbitals is responsible for the unique and diverse properties of the Ln^{3+} ions, and their wavelength maxima do not shift upon change of external conditions, such as temperature, pH, or biological environment, which have encouraged scientists to use them as centres for constructing functional materials.[17] The lanthanide ions suffer from weak light absorption due to the forbidden f-f transitions, a problem that may be overcome by the so-called *antenna* effect (or sensitization). The role of the antenna (usually an organic ligand) is to transfer the energy from the incoming radiation to the lanthanide ions, boosting their luminescence.[18]

Trivalent neodymium plays an important role in near-infrared (1060 nm) light-emitting materials and devices.[19] Such materials find application in the military sector, night-vision illumination sources, consumer electronics, and spectroscopic analysis, especially in optical telecommunication systems.[20] In fact, examples of near-infrared light-emitting lanthanide frameworks are scarce due to both, the presence of high-energy C-H, N-H, and O-H oscillators in the ligands and solvents, which effectively quench non-radiatively the metal excited states, and to the fact that Nd^{3+} has small energy gaps between the ground and the excited electronic states.[21] Eu^{3+} and Tb^{3+} which exhibit, respectively, green and red 4f–4f-emissions are attractive due to their intense, long-lived, sharp emission in the visible region and large energy gap between their main emissive and receiving states, avoiding pronounced vibrational quenching. Eu^{3+} and Tb^{3+} have many important applications including in lasers, phosphors and optical communication amplifiers.[22] Lanthanide-β-diketonate complexes are attractive due to their high-quantum yields and narrow-band emission. These chelates have long been known to give intense emission lines upon UV light irradiation, because of the effective intramolecular energy transfer from the ligands to the central lanthanide ions, which in turn undergo the corresponding radiative emission process.[23]

The synthesis of Ln-based MOFs is, at present, a very active field of research,[24] particularly in view of the possibility of combining microporosity and light emission for fabricating sensor devices for small molecules,[25] anions,[26] cations,[27] gases and vapors,[28] and temperature.[29] Other applications for Ln-MOFs encompass light-emitting devices,[30] multimodal imaging,[31] and drug delivery.[32]

We have been interested in the design of new MOFs with Ln active sites for light-emitting devices. Recently, we have shown that post-synthetic modification of MOFs is an excellent route for preparing infrared and visible-light emitters,[15] and here we wish to extend our studies to other linker modifications, in order to firmly establish the general character of this approach. IsoreticularIRMOF-3 was chosen due to its high porosity and the presence of non-coordinating amino groups on the benzenedicarboxylate linker, which may be easily modified.[33]Thus, the amino group of IRMOF-3 were post-synthetically modified by nucleophilic substitution (chloroacetic acid), nucleophilic addition (glyoxylic acid), reductive amination (glyoxylic acid) and α- and β-additions to α,β-unsaturated carbonyl compounds, and subsequently coordinated to Eu^{3+} and Nd^{3+} ions.

Experimental

1. Materials

2-Aminoterephthalic acid (99%, Aldrich), zinc nitrate hexahydrate (Merck), *N,N*-dimethylformamide (DMF, 99.9%, Aldrich), chloroform (99.5%, Aldrich), acetonitrile (PA, Fisher Scientific), neodymium(III) chloride hexahydrated (99%, Aldrich), europium(III) chloride hexahydrated (99%, Aldrich).

2. Synthesis of IRMOF-3

$Zn(NO_3)_2{\cdot}6H_2O$ (1.795 g, 6 mmol) and 2-aminoterephthalic acid (0.370 g, 2 mmol) were dissolved in DMF (50 mL) at room temperature. The obtained solution was sealed and placed in the oven at 100°C for 18 h. The obtained crystals were separated, washed with DMF (three times), $CHCl_3$ (three times), then immersed into $CHCl_3$ overnight to remove DMF guest molecules from IRMOF-3, and finally stored under $CHCl_3$.

3. Post-synthetic modifications of IRMOF-3

3.1. Synthesis of IRMOF-3-CA

Freshly prepared IRMOF-3 (1.0 g, 3.3 mmol equiv of $–NH_2$) was dispersed in $CHCl_3$ (15 mL). To this mixture, a solution of chloroacetic acid (0.945 g, 10 mmol) and triethylamine (1 mL, 10 mmol) in $CHCl_3$ (15 mL) was added dropwise at room temperature, and the mixture was kept for 48h at room temperature. The crystals were then washed three times with $CHCl_3$ and finally stored under $CHCl_3$.

3.2. Synthesis of IRMOF-3-Gl

IRMOF-3 (1.0 g, 3.3 mmol equiv of $–NH_2$) was dispersed in CH_3CN (15 mL). To this mixture, a solution of glyoxylic acid monohydrate (0.61 g, 6.6 mmol) in CH_3CN (15 mL) was added dropwise at room temperature, and the mixture was sealed and kept for 48 h at room temperature. The crystals were then washed three times with CH_3CN and finally stored under CH_3CN.

3.3. Synthesis of IRMOF-3-Gl-R

Reductive imination using sodium triacetoxyborohydride was performing by dispersing a sample of IRMOF-3-GL (1.2 g) in a vial containing CH_3CN (15 mL). To this mixture, a solution of sodium triacetoxyborohydride (0.250 g, 1 mmol) in CH_3CN (15 mL) was added dropwise at room temperature, and the mixture was heated for 24h at 60 °C. The sample was washed twice with CH_3CN and dried in air.

3.4. Synthesis of IRMOF-3-EM

A toluene solution of diethyl (ethoxymethylene)malonate (0.6 mL, 6 mmol) was added dropwise at room temperature to IRMOF-3 (1.0 g, 3.3 mmol equiv of $–NH_2$) dispersed in toluene (15 mL), and the resulting mixture sealed and kept for 24 h at 80°C. The crystals were then washed three times with toluene and exchange the solvent with $CHCl_3$, finally stored under $CHCl_3$.

3.5. Synthesis of IRMOF-3-MVK (Solid–vapour reactions)

Crystals of IRMOF-3 (1.0 g, 3.3 mmol equiv of $–NH_2$) were transferred inside the conical filter paper of a reactor designed to perform a solid-vapour reaction. Methyl vinyl ketone (MVK) (10 mL) was introduced with the help of a syringe at the bottom of the vessel avoiding any direct contact with the MOF. The system was heated overnight at 200 °C. The yellow IRMOF-3 crystals were washed three times and then soaked in $CHCl_3$ overnight to remove the excess MVK. The product was stored in fresh $CHCl_3$.

4. Complexation with lanthanides

4.1. Synthesis of Ln-IRMOF-3-CA (Ln = Eu, Nd)

A sample of IRMOF-3-CA (1.2 g) was divided equally in two vials containing $CHCl_3$ (15 mL). To this mixture, a solution of $NdCl_3{\cdot}6H_2O$ (0.50 g, 2mmol) in C_2H_5OH (15 mL) or a solution of $EuCl_3{\cdot}6H_2O$ (0.672 g, 2mmol) in C_2H_5OH (15 mL) was added dropwise at room temperature, and the mixture was stand for 3 days. The sample was washed twice with $CHCl_3$ and dried in air.

4.2. Synthesis of Ln-IRMOF-3-GL (Ln= Eu, Nd)

A sample of IRMOF-3-GL (1.2 g) was equally dispersed in two vials containing CH_3CN (15 mL). To this mixture, a solution of $NdCl_3{\cdot}6H_2O$ (0.50 g, 2 mmol) in C_2H_5OH (15 mL) or $EuCl_3{\cdot}6H_2O$ (0.672 g, 2 mmol) in C_2H_5OH (15 mL) was added dropwise at room temperature, and the mixture was stand for 3 days. The sample was washed twice with CH_3CN and dried in air.

4.3. Synthesis of Ln-IRMOF-3-EM (Eu, Nd)

A DMSO (15 mL) solution of $NdCl_3{\cdot}6H_2O$ (250 mg, 1 mmol) or$EuCl_3{\cdot}6H_2O$ (336 mg, 1 mmol) was added dropwise at room temperature to IRMOF-3-EM (340 mg, 1 mmol) dispersed in DMSO (15 mL), being the resulting mixture stand for 3 days. The sample was washed twice with $CHCl_3$ to remove the DMSO molecules from the pores of MOFs, and then dried in air.

4.4. Synthesis of Ln-IRMOF-3-MVK (Eu, Nd).

A DMSO solution (15 mL) of $LnCl_3{\cdot}6H_2O$ (250 mg, 1 mmol (Nd) or 336 mg, 1 mmol (Eu)) [Ln= Eu, Nd] was added dropwise at room temperature to IRMOF-3-MVK (420 mg, 1 mmol) dispersed in DMSO (15 mL), being the resulting mixture stand for 3 days at room temperature. The sample was washed twice with $CHCl_3$ and dried in air.

5. Characterization

Powder X-ray diffraction data were collected on an X'Pert MPD Philips diffractometer (CuKα X-radiation at 40 kV and 50 mA). EDS measurements were carried out on a Hitachi SU-70 fitted with a field emission gun. The optical microscope examinations were carried out on a Leica EZ4HD Digital Microscope-3.0 Megapixel. Fourier transform infrared spectra were measured on a Mattson 5000 in the range 4000-350 cm^{-1} in transmission mode. The pellets were prepared by adding 1-2 mg of MOFs to 200 mg of KBr. The mixture was then carefully mixed and compressed at

a pressure of 10 kPa in order to form transparent pellets. CNH contents were determined on a LECO CHNS-932 elemental analyser. Solution NMR spectra were recorded on Bruker Avance 300 spectrometer (300 MHz) using a solution prepared by digesting 7 mg of sample in d_6-DMSO (500 µL) and dilute DCl (100 µL, 35% DCl). ^{13}C CP/MAS spectra were recorded on a Bruker Avance-400 (DRX) NMR spectrometer operating at 100.6 MHz using a 7 mm CP/MAS Bruker double-bearing probe. All samples were finely ground before packing in the rotors. Rotors were spun at 9 kHz and the spectra were recorded using a 90° pulse length of 4.0 µs, 1 ms contact time and recycle time of 20 s. The photoluminescence spectra were recorded at room temperature on a modular double grating excitation spectrofluorimeter with a TRIAX 320 emission monochromator (Fluorolog-3, Horiba Scientific) coupled to a R928 and H9170 Hamamatsu photomultipliers, respectively, using a front face acquisition mode. The excitation source was a 450 W Xe arc lamp. The emission spectra were corrected for the detection and optical spectral response of the spectrofluorimeter and the excitation spectra were corrected for the spectral distribution of the lamp intensity using a photodiode reference detector. The emission decay curves were measured at room-temperature with a modular double grating excitation spectrofluorimeter with a TRIAX 320 emission monochromator (Fluorolog-3, Horiba Scientific) coupled to a R928, using a pulsed Xe–Hg lamp (6 µs pulse at half width and 20–30 µs tail) or with a Fluorolog TCSPC spectrofluorometer (Horiba Scientific) coupled to a TBX-04 photomultiplier tube module (950 V), 200 ns time-to-amplitude converter and 70 ns delay using a Horiba Scientific pulsed diode (SpectraLED-355, peak at 356 nm) as excitation source .

Results and discussion

Schemes 1 and 2 summarise the post-synthetic modifications of IRMOF-3 carried out by reaction with 2-chloroacetic acid, glyoxylic acid, diethyl (ethoxymethylene)malonate and methyl vinyl ketone. The modified crystals were characterized by powder X-ray diffraction and the results show that the IRMOF-3 framework preserves its identity (Fig. 1).

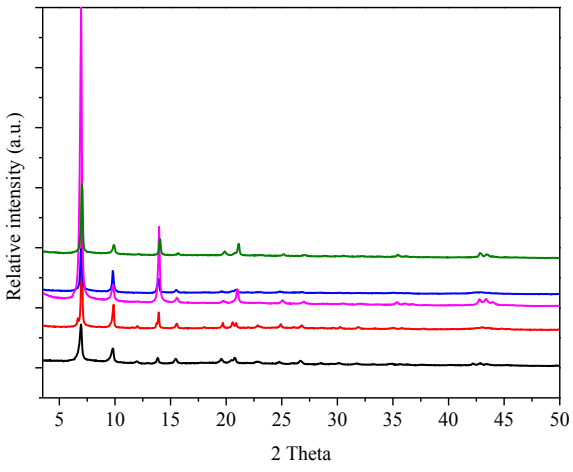

Fig. 1. Powder X-ray diffraction patterns of IRMOF-3(black) and post-synthetically modified materials IRMOF-3-CA(red), IRMOF-3-GL(blue), IRMOF-3-MVK (purple), and IRMOF-3-EM (green).

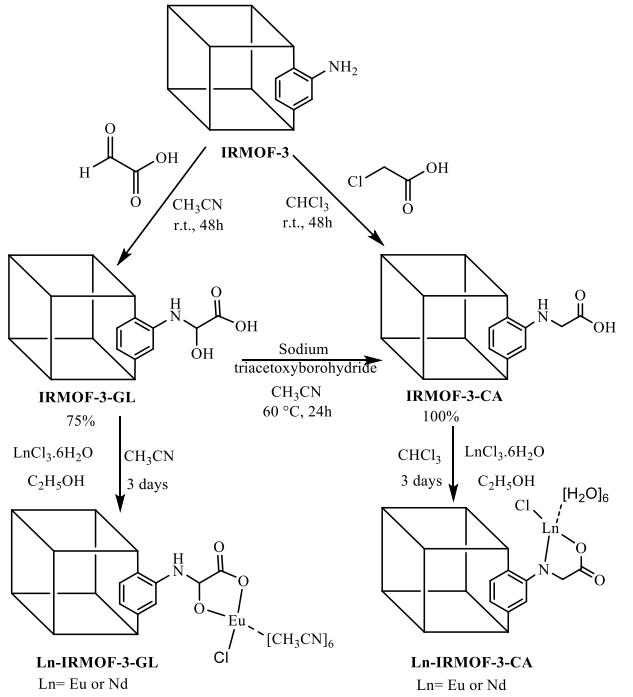

Scheme 1. Post-synthetic covalent modifications of IRMOF-3 with 2-chloroacetic acid (IRMOF-3-CA) and glyoxylic acid (IRMOF-3-GL) and ensuing coordination to Ln^{3+} ions.

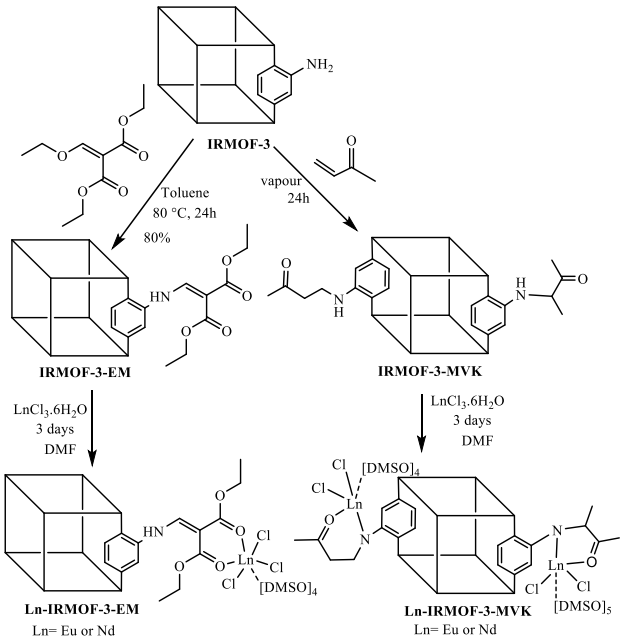

Scheme 2. Post-synthetic covalent modifications of IRMOF-3 with methyl vinyl ketone (IRMOF-3-MVK) and diethyl (ethoxymethylene)malonate (IRMOF-3-EM)and ensuing coordination to Ln^{3+} ions.

The incoming substituent of the linker does not appear in the single crystal X-ray analysis of these modified IRMOF-3 samples probably due to disorder over the four positions on the BDC ligand.[34,35] To overcome this limitation, the crystals were digested in a mixture of d_6-DMSO (500 µL) and dilute DCl (100 µL, 35% DCl) and presented to solution NMR analysis to confirm the presence of the modified benzenedicarboxylate ligand.

1. Synthesis and structure elucidation of IRMOF-3-CA

IRMOF-3-CAresulted from the reaction of IRMOF-3 with 2-chloroacetic acid in chloroform for 48 h at room temperature. The ^{1}H NMR spectrum of IRMOF-3-CA shows signals at δ 7.45 (dd, J 1.6 and 8.2 Hz), 7.80 (d, J 1.6 Hz) and 7.95 (d, J 8.2 Hz) ppm due to the aromatic CH atoms (Fig. 2). The methylene group of IRMOF-3-CA appears as a singlet at δ 4.28 ppm (Fig. S6 andS7).^{1}H NMR shows that the conversion of the amine group was *ca.* 100% since only signals from the modified structure were observed.

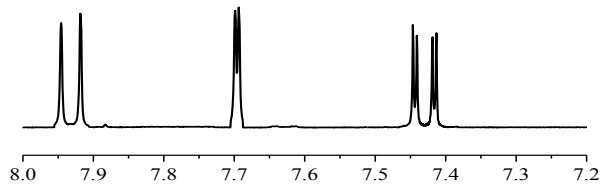

Fig. 2. Aromatic region of the ^{1}H NMR spectrum of IRMOF-3-CA after dissolution in DCl.

The ^{13}C NMR spectrum of IRMOF-3-CA shows signals at δ 43.2 (CH_2), 113.1, 115.3, 117.2, 131.4, 135.7 (aromatic carbons), 150.1 ($C_{aromatic}$-N), 167.2, 168.1 and 169.5 (carboxylates) ppm (Fig. S8). To ensure that the modification occurs within the crystals (and not just on their external surface), the solid-state ^{13}C CP/MAS NMR spectrum was measured and it displays resonances (δ 44.2, 117.9, 133.1, 137.9, 149.6, 173.0 and 176.8 ppm; Fig.S9),similar to those seen in the solution-state spectrum.

The Fourier transform infrared spectrum of IRMOF-3-CA shows intense bands in the region 1578-1616 cm^{-1}, due to the carboxylates, and at 2968, 2878 and 1438 cm^{-1}, assigned to the stretching and bending vibrations of the CH_2group (Fig. S40). CHN analysis confirms the chemical formula $[Zn_4O(C_{10}H_7NO_6)_{3\cdot2}(C_2H_5)_3N)]$(Table S1).

2. Synthesis and structure elucidation of IRMOF-3-GL

The^{1}H NMR spectrum of IRMOF-3-GL show signals atδ7.42 (dd, J1.6 and 8.2 Hz), 7.65 (d, J 1.6 Hz) and 7.92 (d, J8.2 Hz) ppm due to the aromatic protons of the modified material and signals at δ 7.25, 7.56 and 7.96 ppm due to the aromatic protons of the unmodified material (Fig. 3a). The spectrum of IRMOF-3-GL shows a new peak at 5.31 ppm assigned to the methynic proton of the NH-C*H*(OH)-COOH moiety. A 75% conversion of the amine group was calculated by comparing the integration of the signals from the modified material with the sum of both the modified and unmodified IRMOF-3 aromatic signals (Figs. 3a, S10, S11).The^{13}C NMR spectrum of IRMOF-3-GL shows signals at δ 84.1 (CH-OH), 115.3, 118.2, 120.1, 130.5, 135.4(aromatic carbons), 145.2 ($C_{aromatic}$-N), 167.3, 168.4 and 169.5 (carboxylates) ppm for the modified MOF and signals at δ = 113.1, 119.3, 132.5, 136.2(aromatic carbons), 148.4($C_{aromatic}$-N), 166.2 and 167.5 (carboxylates) ppm for the unmodified MOF (Fig. S12). Solid-state ^{13}C CP/MAS NMR shows also the expected main signals (δ 86.0, 159.5, 167.7, 173.0-176.6 ppm) (Fig. S13).

The successful linker modification may also be followed by infrared spectroscopy, namely via the strong absorptions of the carboxylate groups at *ca.* 1627 cm^{-1} (asymmetric stretch) and 1392 cm^{-1} (symmetric stretch),and that at 1578 cm^{-1} due to phenyl ring vibrations. In addition, the –OH bending band appears at 1234 cm^{-1} (Fig. S41).CHN analysis (table S1) confirms the chemical formula $[Zn_4O(C_{10}H_7NO_7)_{2.25}(C_8H_5NO_4)_{0.75}]$.

The available spectroscopic evidence shows that the reaction of glyoxylic acid with the MOF-amino group affords a structure resulting from the addition of the amino group to the aldehyde carbonyl group [Ar-NH-CH(OH)-CO_2H]. However, the elimination of water leading the imine group does not occur.

3. Synthesis and structure elucidation of IRMOF-3-Gl-R

A pseudo-reductive amination of IRMOF-3-Gl was performed using sodium triacetoxyborohydride to afford IRMOF-3-Gl-R. The^{1}H NMR spectrum shows some changes in signals and the aromatic protons of the modified material appear at δ 7.45 (dd, J=1.6 and 8.2 Hz), 7.69 (d, J= 1.6 Hz) and 7.94 (d, J=8.2 Hz) ppm (Fig. 3b). The most important change is the disappearance of the signal at δ 5.31 ppm and appearance of a new resonance at δ 4.28 ppm, assigned to the methylene proton of the NH-CH_2-COOH moiety (Fig. 3b, S14 andS15). This indicates that the addition of triacetoxyborohydride favours the elimination of water and the formation of an imine, which is reduced to the correspondent amine (Scheme S1).

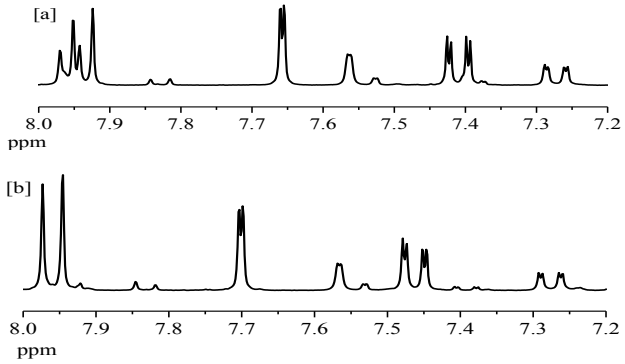

Fig. 3.^{1}H NMR spectra (aromatic region) recorded in DMSO-d_6 after dissolving the modified MOF in DCl of: (a) IRMOF-3-GL, (b) IRMOF-3-GL-R (aliphatic signals are not shown, see S13 for details).

4. Synthesis and structure elucidation of IRMOF-3-EM

Appending diethyl methylenemalonate to IRMOF-3 was accomplished in a 80 % yield by the reaction of the MOF-amino group with diethyl (ethoxymethylene)malonate in dry toluene at 80 °C, for 24h (Scheme 2). The ^{1}H NMR spectrum (Figs. S16-S18) confirms that diethyl (ethoxymethylene)malonate is indeed linked to IRMOF-3 via a tandem Michael addition-elimination process (Scheme 3). The ^{1}H resonances of IRMOF-3-EM appear at δ 1.21 and 1.24 (t, 3H, J 7.1 Hz, CH_3), 4.13 and 4.20 (q, 2H, J 7.1 Hz, CH_2), assigned to the protons of the inequivalent ethyl group, 7.64 (dd, 1H, J 8.2 and 1.3 Hz), 7.86 (d, 1H, J 1.3 Hz), 8.02 (d, 1H, J 8.2 Hz), attributed to the aromatic protons, 8.39 (s, 1H, olefinic-H). ^{13}C NMR also confirms the presence of IRMOF-3 bearing a diethyl methylenemalonate group: δ 14.4 (CH_3), 60.1 (CH_2), 96.6 (quaternary olefinic carbon), 114.3, 116.5, 120.5, 131.7, 136.1, 141.2 (aromatic carbons and olefinic CH), 148.5 ($C_{aromatic}$-N), 165.7, 167.7 and 168.8 (carboxylates) (Fig. S19). All the ^{1}H and ^{13}C assignments were based on 2D NMR

techniques [HMBC (Figs. S20-22) and HSQC (Figs. S23, 24)]. The solid-state ^{13}C CP/MAS NMR spectrum of IRMOF-3-EM further confirms the post-synthetic modification, exhibiting resonances at δ 13.2 and 61.1 ppm due to the ethyl group, and at δ 157.3, 161.2 and 173.5 ppm assigned to the carboxylates (Fig. 4).

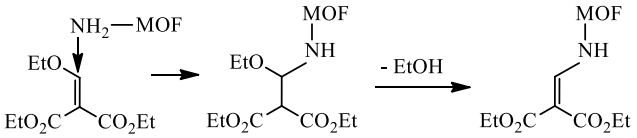

Scheme 3. Reaction of IRMOF-3 with diethyl (ethoxymethylene)-malonate.

The Fourier transform infrared spectrum of IRMOF-3-EM shows intense bands in the region 1623 and 1583 cm^{-1} due to the stretching vibrations of chelated carboxylates and of the phenyl ring, a band at 1685 cm^{-1} attributed to the stretching vibration of the free carboxylate, a band at 3372 cm^{-1} ascribed to the amine proton, and bands at 3100, 2832 and 2649, 1371 cm^{-1} due to the stretching and bending vibrations of CH_2 and C-CH_3 (Fig. S42). CHN analysis (Table S2) confirms the chemical formula $[Zn_4O(C_{16}H_{15}NO_8)_{2.4}(C_8H_5NO_4)_{0.6}]$.

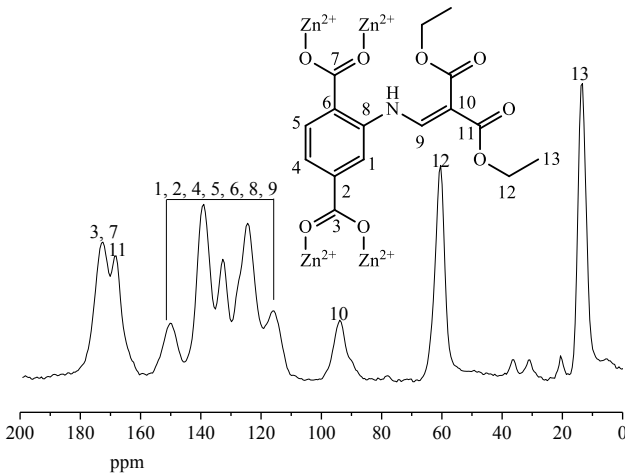

Fig. 4.^{13}C CP/MAS spectrum of IRMOF-3-EM.

5. Synthesis and structure elucidation of IRMOF-3-MVK

Solid–gas and solid–vapour reactions have been studied since the end of the 19th century.[36] More recently these reactions have been applied extensively to organic,[37-41] organometallic[42-45] and metal–organic[46-50] compounds. Such studies have shown that not only dry-medium reactions are possible in a wide range of cases, but also that diverse crystalline forms that are not accessible from solution may be produced when macroscopic solvation is avoided. Finally, they represent a practicable alternative for 'greener' and cheaper industrial processes. Post-synthetic methods aimed at constructing C–N bonds have been intensively studied, in particular the Michael addition of amines to α,β-unsaturated carbonyl compounds. We have devised a synthetic method for the preparation of ketone-terminated IRMOF-3 via the reaction of methyl vinyl ketone vapour with the dry crystals of IRMOF-3. We have realised that we are in the presence of two post-synthetic modifications of IRMOF-3 in a 1:1 proportion: (i) a Michael addition of the MOF-amino group to the methyl vinyl ketone, appending a 3-oxobutyl group, and (ii) the formation of a product resulting from the addition to the α-position of the methyl vinyl ketone. This may be due to the formation of a π complex between the double bond of the methyl ketone and the metal ions of the MOF, favouring the α-addition (Scheme 4).

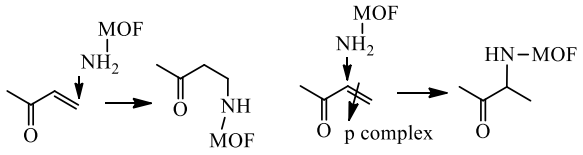

Scheme 4. Reaction of IRMOF-3 with methyl vinyl ketone.

To confirm the formation of the covalently functionalized IRMOF-3-MVK, a wide range of NMR spectra were measured, namely ^1H NMR (Figs. S25-S28), ^{13}C NMR (Fig. S29), ^{13}C CP/MAS (Fig. 6), HSQC (Figs.S30-S32), HMBC (Figs. S33-S36), and 2D COSY (Figs. S37-S39). The structure resulting from the Michael addition to methyl vinyl ketone is supported by the ^1H NMR resonances at δ 2.08 (s, 3H, CH_3), 2.76 (t, 2H, *J* 6.4 Hz, CH_2CO) and 3.35 (t, 2H, *J* 6.4 Hz, CH_2NH), assigned to the aliphatic moiety, and those at 7.02 (d, 1H, *J* 1.4 Hz), 7.07 (dd, 1H, *J* 8.2 and 1.4 Hz), 7.83 (d, 1H, *J* 8.2 Hz) due to the aromatic protons, and the carbon resonances at δ 30.5 (CH_3), 37.5(CH_2NH) and 42.4 (CH_2CO), 112.8, 114.3, 115.4, 132.7, 136.2 (aromatic carbons), 150.5 ($C_{aromatic}$-N), 167.7 and 169.8 (carboxylates), 208.6 (ketone). The structure resulting from the α-addition of the amino-IRMOF-3 to methyl vinyl ketone is confirmed by the ^1H resonances at δ 1.31 (d, 3H, *J* 7.1 Hz, CH_3), 2.52 (s, 3H, $COC\underline{H}_3$), 4.33 (quart, 1H, *J* 7.1 Hz, $C\underline{H}CH_3$), 7.16 (dd, 1H, *J* 8.3 and 1.5 Hz), 7.21 (d, 1H, *J* 1.5 Hz), 7.81 (d, 1H, *J* 8.3 Hz) and the 13C resonances at δ 17.7 (CH_3), 37.2 (CH_3), 57.0 ($C\underline{H}CH_3$), 112.3, 113.9, 117.7, 132.3, 135.7 (aromatic carbons), 148.7 ($C_{aromatic}$-N), 167.8 and 169.1 (carboxylates), 211.3 (ketone). The solid-state ^{13}C CP/MAS NMR spectrum of IRMOF-3-MVK further confirms the post-synthetic modification, as shown in figure 6. The HMBC spectrum unequivocally proves the presence of the described two structures, mainly the connectivity of the $C\underline{H}_2NH$ with the $C_{aromatic}$-N (150.5 ppm) in the case of the Michael adduct and of $C\underline{H}CH_3$with the $C_{aromatic}$-N (148.7 ppm) in the case of the α–addition (Fig. 5).

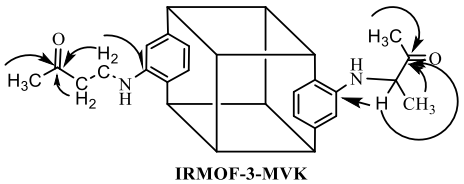

Fig. 5. Main connectivities observed in the HMBC spectrum.

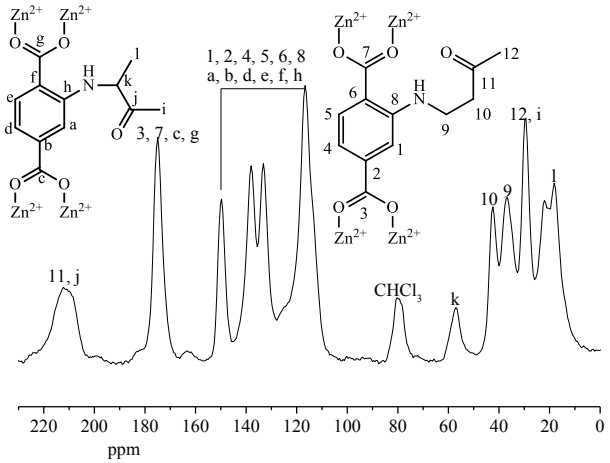

Fig. 6. ^{13}C CP/MAS spectrum of IRMOF-3-MVK.

The Fourier transform infrared spectrum (Fig.S43) presents characteristic intense bands in the region 1623-1583 cm^{-1} due to the stretching vibrations of chelated carboxylates and phenyl ring, a band at 1706 cm^{-1} attributed to the stretching vibration of the free C=O. CHN analysis (Table S1) confirms the chemical formula $[Zn_4O(C_{12}H_{11}NO_5)_{1.38}(C_{12}H_{11}NO_5)_{0.9}(C_8H_5NO_4)_{0.72}]$.

6. Complexation with lanthanides

The pendant groups of the modified IRMOF-3 were used to coordinate Nd^{3+} and Eu^{3+}. To a solution of $NdCl_3.6H_2O$ or $EuCl_3 \cdot 6H_2O$ in ethanol was added to IRMOF-3-CA dispersed in chloroform, IRMOF-3-Gl dispersed in acetonitrile and the resulting mixtures were allowed to stand at room temperature for 3 days (Scheme 1), while a solution of $NdCl_3 \cdot 6H_2O$ or $EuCl_3 \cdot 6H_2O$ in DMSO was added to crystals of IRMOF-3-EM or IRMOF-3-MVK (Scheme 2). These different procedures are due to the stability of these structures, only the latter being stable in air. Powder X-ray diffraction showed that the framework and crystallinity of the MOFs were preserved upon Ln chelation (Fig. S1-S4).

The crystal morphology of Ln^{3+}-IRMOF-3-CA, Ln^{3+}-IRMOF-3-Gl, Ln^{3+}-IRMOF-3-EM and Ln^{3+}-IRMOF-3-MVK was determined by scanning electron microscopy and optical microscopy (Figs. S44-S47). As observed for previous IRMOF-3 samples, these materials exhibit a cubic habit. The presence of Ln ions and the composition of the materials were determined by energy dispersive X-ray spectroscopy analysis of 10 crystals (Tables S1 and S2).

6.1. Ln^{3+}-IRMOF-3-CA

The comparison of the infrared spectra of Nd-IRMOF-3-CA, Eu-IRMOF-3-CA and IRMOF-3-CA show significant differences. The CH_2 group of IRMOF-3-CA displays two intense bands at 2984, 3031 cm^{-1} corresponding to the symmetric and asymmetric stretching modes, but only one in Ln-IRMOF-3-CA 2984 cm^{-1}; the pair of bands assigned to ring CH modes at 3062 and 3078 $cm^{-1}$are replaced by a broad and mostly symmetrical single band at 3075 cm^{-1}. The C=O stretching vibration appearing as a shoulder in IRMOF-3-CA at 1683 cm^{-1} is shifted to lower (60 cm^{-1}) wavenumbers in the complexes indicating the participation of carboxylates in the chelation of Ln^{3+}. New bands are found in the spectra of Nd-IRMOF-3-CA at 582and 487 cm^{-1} and assigned to Ln–OCO and Ln–N stretching vibrations (Fig. S40). Therefore, it is concluded that IRMOF-3-CA coordinates with Ln^{3+} ions via its deprotonated carboxylated and the amino groups. EDS analysis showed that the molar ratio of Zn^{2+} to $Ln^{3+}$was 4:3 and of Ln^{3+} to Cl was 1:1. CHN analysis and EDS confirm the chemical formula of Ln-IRMOF-3-CA as $[Zn_4O(C_{10}H_5NO_6LnCl \cdot 6H_2O)_3$, Ln= Eu or Nd].

6.2. Ln^{3+}-IRMOF-3-GL

The Fourier transform infrared spectrum spectra of IRMOF-3-GL and Ln-IRMOF-3-GL are similar, with small intensity variations in a few bands. The spectra are dominated by the strong absorptions of the carboxylate groups, around 1620 cm^{-1} (asymmetric stretch) and 1392 cm^{-1} (symmetric stretch). In addition, the intensity reduction of the broad band at ca. 1250 cm^{-1} is consistent with a change in the –OH bending mode. A new band is found in the spectra of Ln-IRMOF-3-GL at 385cm^{-1} assigned to (Ln–N) stretching vibrations (Fig. S41). Energy dispersive X-ray analysis gives a ratio Zn^{2+} to Nd^{3+} of 4:2.25 and together with CHN analysis confirms the chemical formula $[Zn_4O(C_{22}H_{23}N_7O_7LnCl)_{2.25}(C_8H_5NO_4)_{0.75}]$.

6.3. Ln^{3+}-IRMOF-3-EM

As most β-diketonates may coordinate Ln^{3+} ions forming stable complexes, the terminated β-diketonate IRMOF-3-EM was mixed with $LnCl_3 \cdot 6H_2O$, in DMSO. Because MOFs functionalization is partial, the amount of malonate moieties and Ln-β-diketonate complex anions is too low to allow observation of their characteristic Fourier transform infrared bands (Fig. S42). Fortunately, the successful attachment of Ln^{3+} ions to MOF backbones is strongly supported by the symmetrical vibration of two C=O links in the resonating structure of the coordinated β-diketonate ligands around 1535 cm^{-1}, which is similar to peak in the spectrum of the modified IRMOF-3-EM. Energy dispersive X-ray spectroscopy provides positive evidence for the successful functionalization of MOF with Ln^{3+} ions (Table S2) and together with CHN analysis confirms the chemical formula of Eu-IRMOF-3-EM to be $[Zn_4O(C_{37}H_{64}N_8O_{15}Eu)_{2.4}(C_8H_5NO_4)_{0.6}]$ and that of Nd-IRMOF-3-EM $[Zn_4O(C_{37}H_{64}N_8O_{15}Nd)_{2.4}(C_8H_5NO_4)_{0.6}]$.

6.4. Ln^{3+}-IRMOF-3-MVK

A solution of $LnCl_3 \cdot 6H_2O$ [Ln= Eu, Nd] in DMSO was added dropwise at room temperature to IRMOF-3-MVK. Infrared spectroscopy confirms the successful Ln chelation (Fig. S43): the spectrum of Ln-IRMOF-3-MVKshows the characteristic symmetric and asymmetric stretching vibrations from the deprotonated carboxylic acids at 1313 and 1580 cm^{-1}, respectively. The band of the aromatic benzene vibration appears at 1512 cm^{-1}.The large bands at 1006 and 960 cm^{-1} are due to, respectively, S-O and C-S stretching of the coordinated DMSO. Additional evidence for this chelation reaction was obtained by energy dispersive X-ray spectroscopy and CHN analysis, confirming the chemical formula of Eu-IRMOF-3-MVK to be $[Zn_4O(C_{22}H_{40}NS_5O_{10}EuCl_2)_{1.38}(C_{22}H_{40}NS_5O_{10}EuCl_2)_{0.9}(C_8H_5NO_4)_{0.72}]$ and that of Nd-IRMOF-3-MVK $[Zn_4O(C_{22}H_{40}NS_5O_{10}NdCl_2)_{1.38}(C_{22}H_{40}NS_5O_{10}NdCl_2)_{0.9}(C_8H_5NO_4)_{0.72}]$.

7. Photoluminescence properties

Figure 7 shows the emission spectra of the Eu^{3+}-containing MOFs. The spectra consist of a series of intra-4f transitions, assigned to the $^5D_0 \rightarrow {}^7F_{0\text{-}4}$ transitions of the Eu^{3+} ion, and a broad band ascribed to the hybrid host (since it is also seen in the undoped samples, Fig. S48). A very similar band has been reported for Ln^{3+}-complexes of β–diketonates bearing aromatic ligands and assigned to π–π^* and/or n-π^*transitions. [51]

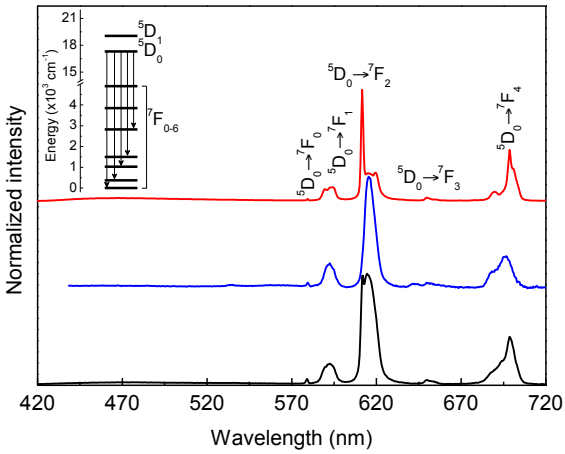

Fig. 7. Emission spectra of Eu-IRMOF-3-EM (black), Eu-IRMOF-3-MVK (red), and Eu-IRMOF-3-GL (blue) excited at 365 nm. The inset depicts part of the energy level scheme of Eu^{3+} ions.

For Eu-IRMOF-3-CA the host band is quite intense indicating an inefficient ligand-to-metal energy transfer (Fig. S49). In contrast, for Eu-IRMOF-3-EM, Eu-IRMOF-3-MVK and Eu-IRMOF-3-GL this band is very faint indicating that an efficient energy transfer from these matrices to the Eu^{3+} ions boosts the light emission. Furthermore, the $^7F_{1\text{-}4}$ Stark level splitting is better observed in Eu-IRMOF-3-MVK, relatively to that of the other two MOFs, due to a smaller dispersion of closely similar Eu^{3+} local neighbourhoods. The corresponding excitation spectra (Figure 8) display broad bands, ascribed to the ligands, overlapping with a series of narrow intra-4f lines. The higher relative intensity of the broad bands for Eu-IRMOF-3-MVK and Eu-IRMOF-3-EM indicates that the ligands sensitization process is more effective in this case.

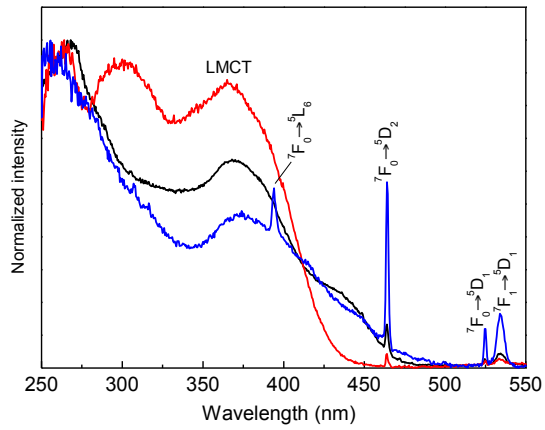

Fig. 8. Excitation spectra of Eu-IRMOF-3-EM (black), Eu-IRMOF-3-MVK (red) and Eu-IRMOF-3-GL (blue) at 615 nm. The peak at 375 nm is ascribed to the $\pi \rightarrow \pi^*$ band of the benzene ring. The wide band is assigned to the ligand-metal charge transfer.

It is of interest to optimize the near infrared emission by changing the nature of the pendant organic moiety. All Nd^{3+}-containing MOFs show emission at 1064 nm ($^4F_{3/2} \rightarrow {}^4I_{11/2}$) and 1330 nm ($^4F_{3/2} \rightarrow {}^4I_{13/2}$) (Fig. 9), excited via both the hybrid host and intra-$4f^3$ lines (Fig. S48). No significant changes are observed in the energy and full-width-at-half-maximum (FWHM) of the lines of the Nd-IRMOF-3-EM, Nd-IRMOF-3-MVK and Nd-IRMOF-3-CA materials. For Nd-IRMOF-3-GL, however, the FWHM of the $^4F_{3/2} \rightarrow {}^4I_{13/2}$ transition is lower (*ca.* 20 nm, 30 nm in the other MOFs) and the $^4F_{3/2} \rightarrow {}^4I_{13/2}$ transition displays a relatively low intensity.

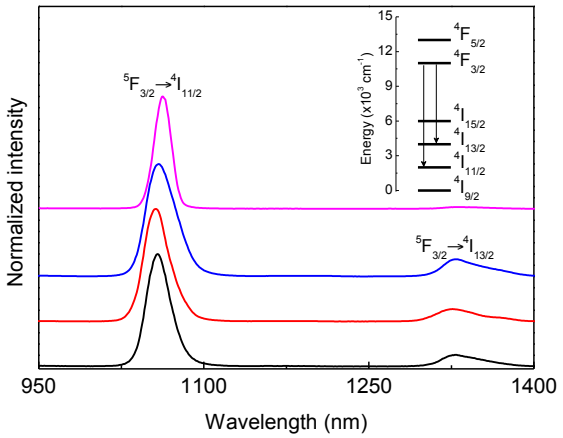

Fig. 9. Near infrared emission spectra of Nd-IRMOF-3-EM (black), Nd-IRMOF-3-MVK (red), Nd-IRMOF-3-CA (blue) and Nd-IRMOF-3-GL (purple) excited at 378 nm, 395 nm, 365 nm and 527 nm, respectively. The inset depicts part of the energy level scheme of Nd^{3+} ions. The $^4F_{3/2}$ energy level is populated via the ligands excited states.

The corresponding excitation spectra (Figure 10) display a broad band in the high-energy region of the spectrum ascribed to the ligands, overlapping with a series of narrow intra-$4f^3$ lines. The higher relative intensity of the broad emission for Nd-IRMOF-3-MVK indicates that the sensitization process is more effective in this case. Nevertheless, because the near-infrared emission is observed for excitation of both the hybrid host and intra-4f transitions, all the modified MOFs are good matrices for absorbing energy and transferring it to the Nd^{3+} ions.

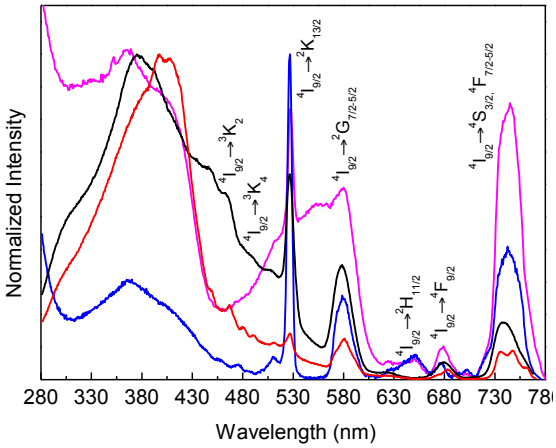

Fig. 10. Excitation spectra of Nd-IRMOF-3-EM (black), Nd-IRMOF-3-MVK (red), Nd-IRMOF-3-CA (blue) and Nd-IRMOF-3.

The luminescence emission decays of Nd-IRMOF-3-GL, Nd-IRMOF-3-MVK and Nd-IRMOF-3-CA were recorded at room temperature (Fig. S51) and the lifetimes are listed on table 1. The quantum yield (QY) is very low (1%) for all Nd^{3+} doped materials. The $^5D_0$ lifetime of Eu-IRMOF-3-GL, Eu-IRMOF-3-MVK, Eu-IRMOF-3-CA and Eu-IRMOF-3-EM are shown in table 1 and the emission decay curves in figure S52. The synthesised hybrid materials doped with Eu^{3+} have a low quantum yield (1%).

Table 1 Lifetime values obtained at 300 K under distinct excitation wavelengths (λ_{ex}, nm) .

Material	Exc (nm)	lifetime (ms)
Nd-IRMOF-3-MVK	395	0.012±0.001
Nd-IRMOF-3-GL	365	0.011±0.001
Nd-IRMOF-3-CA	365	0.012±0.001
Eu-IRMOF-3-GL	420	0.125±0.002
Eu-IRMOF-3-CA	380	0.173±0.006
Eu-IRMOF-3-EM	355	0.310±0.001
Eu-IRMOF-3-MVK	355	0.331±0.001

Conclusion

We have successfully developed visible and near-infrared emitting lanthanide-organic frameworks using the post-synthetic modification technique. This method has the advantage of preserving the original MOFs structure with the addition of new properties, combining the microporosity of the MOFs host and the functionality of lanthanide ions. Furthermore, photoluminescence studies showed that the post-synthetic modified MOF was able to sensitise the Ln^{3+} ions (antenna effect) leading to characteristic emission in the near infrared and visible regions.

Acknowledgements

This work was developed in the scope of the project CICECO-Aveiro Institute of Materials (Ref. FCT UID /CTM /50011/2013) and Organic Chemistry Research Unit (QOPNA) (project PEst-C/QUI/UI0062/2013), financed by national funds through the FCT/MEC and when applicable co-financed by FEDER under the PT2020 Partnership Agreement. We also thank the Portuguese National NMR Network (RNRMN). Rute A. S. Ferreira is gratefully acknowledged for her help with the photoluminescence measurements. RMA thanks also FCT for the PhD research grant (SFRH/BD/51269/2010). We further acknowledge COST Action MP1202.

Notes and references

[a]*Department of Chemistry, CICECO, University of Aveiro, 3810-193 Aveiro, Portugal. e-mail: rocha@ua.pt*
[b]*Department of Chemistry, QOPNA, University of Aveiro, 3810-193 Aveiro, Portugal. e-mail: artur.silva@ua.pt*
[c]*Department of Physics, CICECO, University of Aveiro, 3810-193 Aveiro, Portugal. e-mail:lcarlos@ua.pt*
† Electronic Supplementary Information (ESI) available: Experimental procedures, analytical data, and NMR spectra.
SeeDOI: 10.1039/b000000x/

1. H. Li, M. Eddaoudi, M. O'Keeffe, O. M. Yaghi, *Nature,* 1999, **402**, 276-279.
2. O. M. Yaghi, G. Li, H. Li, *Nature,* 1995, **378**, 703 – 706.
3. J. Y. Lee, O. K. Farha, J. Roberts, K. A. Scheidt, S. B. T. Nguyen, J. T. Hupp, *Chem. Soc. Rev.*, 2009, **38**, 1450-1459.
4. a) Y. Ikezoe, G. Washino, T. Uemura, S. Kitagawa, H. Matsui, *Nature Mat.*, 2012, **11**, 1081-1085. b) Y. Chen, V. Lykourinou, C. Vetromile, H. Tran, L.-J. Ming, R. W. Larsen, S. Ma, *J. Am. Chem. Soc.*, 2012, **134**, 13188-13191. c) V. Lykourinou, Y. Chen, X.-S. Wang, L. Meng, H. Tran, L.-J. Ming, R. L. Musselman, S. Ma, *J. Am. Chem. Soc.*, 2011, **133**, 10382-10385. d) W.-L. Liu, S.-H. Lo, B. Singco, C.-C. Yang, H.-Y. Huang, C.-H. Lin, *J. Mat. Chem. B*, 2013, **1**, 928-932. e) Y.-H. Shih, S.-H. Lo, N.-S. Yang, B. Singco, Y.-J. Cheng, C.-Y. Wu, I. H. Chang, H.-Y. Huang, C.-H. Lin, *ChemPlusChem*, 2012, **77**, 982-986. f) C. M. Doherty, G. Grenci, R. Riccò, J. I. Mardel, J. Reboul, S. Furukawa, S. Kitagawa, A. J. Hill, P. Falcaro, *Adv. Mat.*, 2013, **25**, 4701-4705.
5. a) R. B. Getman, Y.-S. Bae, C. E. Wilmer, R. Q. Snurr, *Chem. Rev.,* 2012, **112**, 703-723. b) K. Sumida, D. L. Rogow, J. A. Mason, T. M. McDonald, E. D. Bloch, Z. R. Herm, T.-H. Bae, J. R. Long, *Chem. Rev.*, 2012, **112**, 724-781. c) M. P. Suh, H. J. Park, T. K. Prasad, D.-W. Lim, *Chem. Rev.*, 2012, **112**, 782-835. d) J.-R. Li, J. Sculley, H.-C. Zhou, *Chem. Rev.*, 2012, **112**, 869-932.
6. a) N. L. Rosi, J. Eckert, M. Eddaoudi, D. T. Vodak, J. Kim, M. O'Keeffe,O. M. Yaghi, *Science*, 2003, **300**, 1127-1129. b) S. Ma, H.-C. Zhou, *Chem. Commun.*, 2010, **46**, 44-53. c) L. J. Murray, M. Dincă, J. R. Long, *Chem. Soc. Rev.*, 2009, **38**, 1294-1314.
7. a) P. Horcajada, T. Chalati, C. Serre, B. Gillet, C. Sebrie, T. Baati, J. F. Eubank, D. Heurtaux, P. Clayette, C. Kreuz, J.-S. Chang, Y. K. Hwang, V. Marsaud, P.-N. Bories, L. Cynober, S. Gil, G. Ferey, P. Couvreur, R. Gref, *Nat. Mat.*, 2010, **9**,

172-178. b) J. Della Rocca, D. Liu, W. Lin, *Acc. Chem. Res.*, 2011, **44**, 957-968. c) P. Horcajada, R. Gref, T. Baati, P. K. Allan, G. Maurin, P. Couvreur, G. Ferey, R. E. Morris, C. Serre, *Chem. Rev*., 2012, **112**, 1232-1268.

8. a) D. Buso, J. Jasieniak, M. D. H. Lay, P. Schiavuta, P. Scopece, J. Laird, H. Amenitsch, A. J. Hill, P. Falcaro, *Small*, 2012, **8**, 80-88. b) B. Liu, *J. Mat. Chem*., 2012, **22**, 10094-10101. c) L. E. Kreno, K. Leong, O. K. Farha, M. Allendorf, R. P. Van Duyne, J. T. Hupp, *Chem. Rev*., 2012, **112**, 1105-1125. d) C. Wang, T. Zhang, W. B. Lin, *Chem. Rev*., 2012, **112**, 1084-1104.

9. a) S. M. Cohen, *Chem. Rev.,* 2012, **112**, 970–1000. b) K. K. Tanabe, S. M. Cohen, *Chem. Soc. Rev*. 2011, **40**, 498–519. c) S. M. Cohen, *Chem. Sci.*, 2010, **1**, 32–36. d) Z. Wang, S. M. Cohen, *Chem. Soc. Rev.*, 2009, **38**, 1315–1329.

10. Z. Wang, S. M. Cohen, *J. Am. Chem. Soc.,* 2009, **131**, 16675–16677.

11. a) T. M. McDonald, D. M. D'Alessandro, R. Krishna, J. R. Long, *Chem. Sci.,* 2011, **2**, 2022–2028. b) Z. Wang, S. M. Cohen, *J. Am. Chem. Soc.,* 2009, **131**, 16675–16677.

12. Y. K. Hwang, D.-Y. Hong, J.-S. Chang, S. H. Jhung, Y.-K. Seo, J. Kim, A. Vimont, M. Daturi, C. Serre, G. Férey, *Angew. Chem. Int. Ed.,* 2008, **47**, 4144–4148.

13. T. Gadzikwa, O. K. Farha, C. D. Malliakas, M. G. Kanatzidis, J. T. Hupp, S. T. Nguyen, *J. Am. Chem. Soc*., 2009, **131**, 13613–13615.

14. K. M. L. Taylor-Pashow, J. D. Rocca, Z. Xie, S. Tran, W. Lin, *J. Am. Chem. Soc.,* 2009, **131**, 14261–14263.

15. a) R. M. Abdelhameed, L. D. Carlos, A. M. S. Silva, J. Rocha, *Chem. Commun*. 2013, **49**, 5019-5021. b) R. M. Abdelhameed, L. D. Carlos, P. Rabu, S. M. Santos, A. M. S. Silva, J. Rocha, *Eur. J. Inorg. Chem*. 2014, **31**, 5285-5295. c) Y. Zhou, B. Yan, F. Lei, *Chem. Commun*.2014, **50**, 15235-15238.

16. J.-C. G. Bünzli, C. Piguet, *Chem. Soc. Rev.*, 2005, **34**, 1048-1077

17. J. Kido, Y. Okamoto, *Chem. Rev.,* 2002, **102**, 2357-2368.

18. D. Parker, *Coord. Chem. Rev.,* 2000, **205**,109–130.

19. L. H. Slooff, A. Polman, F. Cacialli, R. H. Friend, G. A. Hebbink, F. C. J. M. van Veggel, D. N. Reinhoudt, *Appl. Phys. Lett.,*2001,**78**, 2122-2124.

20. a) J. H. Kim, P. H. Holloway, *Adv. Mater.,* 2005, **17**, 91-96. b) J. Zhang, C. M. Shade, D. A. Chengelis, S. Petoud, *J. Am. Chem. Soc*., 2007, **129**, 14834-14835. c) X. Q. Lu, W. X. Feng, Y. N. Hui, T. Wei, J. R. Song, S. S. Zhao, W. Y. Wong, W. K. Wong, R. A. Jones, *Eur. J. Inorg. Chem*., 2010, 2714-2722.

21. S. V. Eliseeva, J.-C. G. Bünzli, *Chem. Soc. Rev.,* 2010, **39**, 189-227.

22. a) H. G Liu,. Y. Lee, W. P. Qin, K. Jang, S. Kim, X. S. Feng, *J. Appl. Polym. Sci*., 2004, **92**, 3524-3530. b) Y. Hasegawa, M. Yamamuro, Y. Wada, N. Kanehisa, Y. Kai, S. Yanagida, *J. Phys. Chem. A*, 2003, **107**, 1697-1702.c) K. Kuriki, Y. Koike, *Chem. Rev.,* 2002, **102**, 2347-2356.

23. S. Sato, M. Wada, *Bull. Chem. Soc. Jpn*., 1970, **43**, 1955-1962.

24. a) Y. Cui, Y. Yue, G. Qian, B. Chen, *Chem. Rev*., 2012, **112**, 1126-1162. b) J. Rocha, L. D. Carlos, F. A. A. Paz,D. Ananias, *Chem. Soc. Rev*., 2011, **40**, 926-940. c) M. D. Allendorf, C. A. Bauer, R. K. Bhaktaa, R. J. T. Houk, *Chem. Soc. Rev*., 2009, **38**, 1330-1352.

25. a) B. Chen, Y. Yang, F. Zapata, G. Lin, G. Qian, E. B. Lobkovsky, *Adv. Mater.*, 2007, **19**, 1693-1696. b) Y. Bai, G.-J. He, Y.-G. Zhao, C.-Y. Duan, D.-B. Dang, Q.-J. Meng, *Chem. Commun*., 2006, 1530-1532. c) E. Y. Lee, S. Y. Jang, M. P. Suh, *J. Am. Chem. Soc.,* 2005, **127**, 6374-6381.

26. a) B. Chen, L. Wang, F. Zapata, G. Qian, E. B. Lobkovsky, *J. Am. Chem. Soc.*, 2008, **130**, 6718-6719. b) K. L. Wong, G. L. Law, Y. Y. Yang, W. T. Wong, *Adv. Mater.*, 2006, **18**, 1051-1054.

27. a) B. Zhao, X.-Y. Chen, Z. Chen, W. Shi, P. Cheng, S.-P. Yan, D.-Z. Liao, *Chem. Commun*., 2009, 3113-3115. b) X.-Q. Zhao, B. Zhao, W. Shi, P. Cheng, *Cryst. Eng. Comm*., 2009, **11**, 1261-1269. c) B. Zhao, X.-Y. Chen, P. Cheng, D.-Z. Liao, S.-P. Yan, Z.-H. Jiang, *J. Am. Chem. Soc*., 2004, **126**, 15394-15395. d) W. Liu, T. Jiao, Y. Li, Q. Liu, M. Tan, H. Wang, L. Wang, *J. Am. Chem. Soc.*, 2004, **126**, 2280-2281.

28. a) J. An, C. M. Shade, D. A. Chengelis-Czegan, S. Petoud, N. L. Rosi, *J. Am. Chem. Soc.,* 2011, **133**, 1220-1223. b) B. V. Harbuzaru, A. Corma, F. Rey, P. Atienzar, J. L. Jordá, H. Garcia, D. Ananias, L. D. Carlos, J. Rocha, *Angew. Chem., Int. Ed.,* 2008, **47**, 1080-1083.

29. A. Cadiau, C. D. S. Brites, P. M. F. J. Costa, R. A. S. Ferreira, J. Rocha, L. D. Carlos, *ACS Nano,* 2013, **7**, 7213-7218.

30. a) K. A. White, D. A. Chengelis, M. Zeller, S. J. Geib, J. Szakos, S. Petoud, N. L. Rosi, *Chem. Commun*., 2009, 4506-4508. b) K. A. White, D. A. Chengelis, K. A. Gogick, J. Stehman, N. L. Rosi, S. Petoud, *J. Am. Chem. Soc*., 2009, **131**, 18069-18071. c) B. Chen, Y. Yang, F. Zapata, G. Qian, Y. Luo, J. Zhang, E. B. Lobkovsky, *Inorg. Chem.* 2006, **45**, 8882-8886.

31. a) W. Lin, W. J. Rieter, K. M. L. Taylor, *Angew. Chem., Int. Ed.,* 2009, **48**, 650-658. b) K. M. L. Taylor, A. Jin, W. Lin, *Angew. Chem., Int. Ed.,* 2008, **47**, 7722-7725. c) W. J. Rieter, K. M. L. Taylor, W. Lin, *J. Am. Chem. Soc.*, 2007, **129**, 9852-9853. d) W. J. Rieter, Taylor, H. An, W. Lin, W. Lin, *J. Am. Chem. Soc.,* 2006, **128**, 9024-9025.

32. K. M. L. Taylor-Pashow, J. D. Rocca, Z. Xie, S. Tran, W. Lin, *J. Am. Chem. Soc.*, 2009, **131**, 14261-14263.

33. Z. Wang, S. M. Cohen, *Angew. Chem.,* 2008, **120**, 4777-4780.

34. M. Eddaoudi, J. Kim, N. Rosi, D. Vodak, J. Wachter, M. O'Keeffe, O.M. Yaghi, *Science*, 2002, **295**, 469-472.

35. J. S. Costa, P. Gamez, C. A. Black, O. Roubeau, S. J. Teat, J. Reedijk, *Eur. J. Inorg. Chem.,* 2008, 1551-1554.

36. G. Pellizzari,*Gazz. Chim. Ital*., 1884, **18**, 14–362.

37. D. Braga, F. Grepioni, L. Maini, K. Rubini, M. Polito, R. Brescello, L. Cotarca, M. T. Duarte, V. Andre, M. F. M. Piedade, *New J.Chem*., 2008, **32**, 1788–1795.

38. G. Kaupp, *Organic Solid State Reactions*, ed. F. Toda, Springer, Berlin, Heidelberg, 2005, **254**, 130–131.

39. G. Kaupp, J. Schmeyers, J. Boy, *Chem. A Eur. J.,* 1998, **4**, 2467–2474.

40. K. Tanaka, D. Fujimoto, T. Oeser, H. Irngartinger, F. Toda, *Chem. Commun*., 2000, 413–414.
41. K. Tanaka, F. Toda, *Chem. Rev*., 2000, **100**, 1025–1074.
42. M. Albrecht, M. Lutz, A. L. Spek, G. van Koten, *Nature*, 2000, **406**, 970–974.
43. M. Albrecht, R. A. Gossage, M. Lutz, A. L. Spek, G. van Koten, *Chem. Eur. J.,* 2000, **6**, 1431–1445.
44. G. Kaupp, M. R. Naimi-Jamal, L. Maini, F. Grepioni, D. Braga, *Cryst. Eng. Comm.*, 2003, **5**, 474–479.
45. D. Braga, F. Grepioni, M. Polito, M. R. Chierotti, S. Ellena, R. Gobetto, *Organometallics*, 2006, **25**, 4627–4633.
46. C. J. Adams, H. M. Colquhoun, P. C. Crawford, M. Lusi, A. G. Orpen, *Angew. Chem., Int. Ed*., 2007, **46**, 1124–1128.
47. C. J. Adams, M. F. Haddow, M. Lusi, A. G. Orpen, *Proc. Natl. Acad. Sci. U. S. A*., 2010, **107**, 16033–16038.
48. C. J. Adams, M. A. Kurawa, M. Lusi and A. G. Orpen, *Cryst. Eng. Comm.*, 2008, **10**, 1790–1795.
49. G. M. Espallargas, M. Hippler, A. J. Florence, P. Fernandes, J. van de Streek, M. Brunelli, W. I. F. David, K. Shankland, L. Brammer, *J. Am. Chem. Soc*., 2007, **129**, 15606–15614.
50. G. M. Espallargas, J. van de Streek, P. Fernandes, A. J. Florence, M. Brunelli, K. Shankland and L. Brammer, *Angew. Chem., Int. Ed*., 2010, **49**, 8892–8896.
51. G. Zucchi, *Intl. J. Inorg. Chem.*, 2011, article ID 918435.

